

1 **Comparison of linear combination modeling strategies for GABA-edited MRS**
2 **at 3T**

3 Helge J. Zöllner^{1,2}, Sofie Tapper^{1,2}, Steve C. N. Hui^{1,2}, Peter B. Barker^{1,2}, Richard A. E. Edden^{1,2},

4 Georg Oeltzschner^{1,2,*}

5 ¹ *Russell H. Morgan Department of Radiology and Radiological Science, The Johns Hopkins*

6 *University School of Medicine, Baltimore, MD, United States*

7 ² *F. M. Kirby Research Center for Functional Brain Imaging, Kennedy Krieger Institute, Balti-*

8 *more, MD, United States*

9

10 ***Corresponding author:**

11 Georg Oeltzschner, Ph.D.

12 Division of Neuroradiology, Park 367G

13 The Johns Hopkins University School of Medicine

14 600 N Wolfe St

15 Baltimore, MD 21287

16 goeltzs1@jhmi.edu

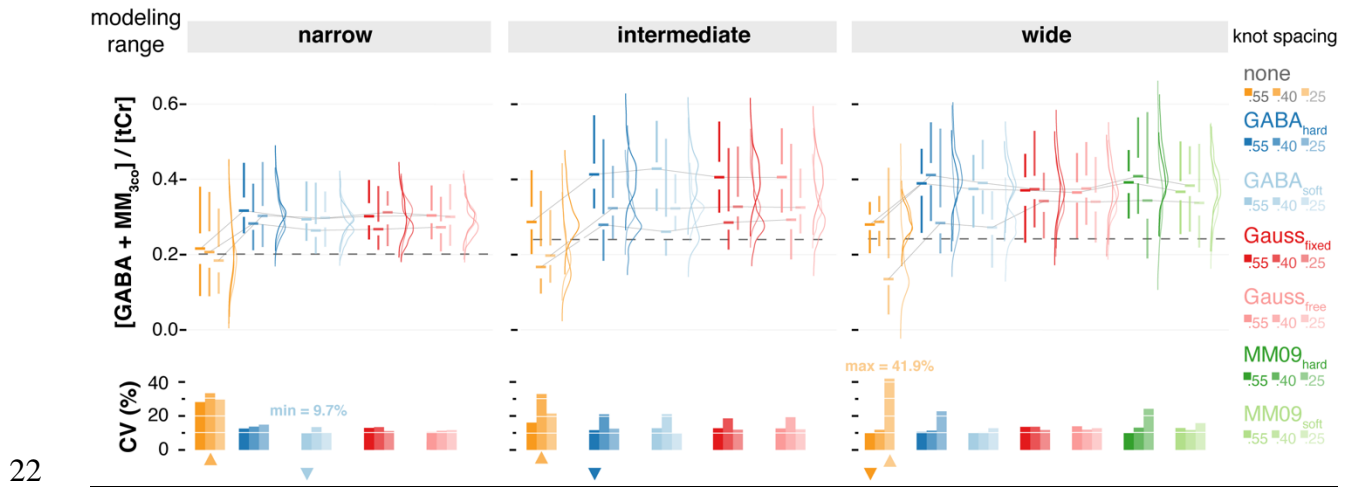
17

18

19 *Running title: Linear combination modeling of GABA-edited MRS*

20 *Word count: 7420*

21 Graphical Abstract



23 102 strategies to model GABA-edited MRS with linear combination
24 modeling were evaluated to quantify GABA and GABA+ in Osprey.
25 Significantly different GABA and GABA+ estimates were found when a
26 well-parameterized macro-molecule at 3 ppm was included. The
27 findings suggest that linear combination modeling needs to be adapted
28 for quantification of GABA-edited MRS.
29

30 **Abbreviations**

31 γ -aminobutyric-acid – GABA; Linear combination modeling – LCM; macromolecule – MM;
32 GABA + MM - GABA+; homocarnosine – HCar; glutamate – Glu; glutamine – Gln; glutathione
33 – GSH; N-acetylaspartylglutamate – NAAG; N-acetylaspartate – NAA; Hankel singular value
34 decomposition – HSVD; full-width at half-maximum – FWHM; creatine – Cr; negative creatine
35 methylene – -CrCH₂; phosphocreatine – PCr; SD – standard deviation; Akaike Information Cri-
36 terion – AIC; SSE – sum of squared error; coefficients of variation – CVs;

37

38

39 **Keywords**

- 40 • Magnetic resonance spectroscopy
- 41 • Linear combination modeling
- 42 • GABA-edited MEGA-PRESS

43 Abstract

44 Purpose

45 J-difference-edited spectroscopy is a valuable approach for the in vivo detection of γ -
46 aminobutyric-acid (GABA) with MRS. A recent expert consensus article recommends linear
47 combination modeling (LCM) of edited MRS but does not give specific details of implementa-
48 tion. This study explores different modeling strategies to adapt LCM for GABA-edited MRS.

49 Methods

50 61 medial parietal lobe GABA-edited MEGA-PRESS spectra from a recent 3T multi-site study
51 were modeled using 102 different strategies combining six different approaches to account for
52 co-edited macromolecules, three modeling ranges, three baseline knot spacings, and the use of
53 basis sets with or without homocarnosine. The resulting GABA and GABA+ estimates (quanti-
54 fied relative to total creatine), the residuals at different ranges, SDs and CVs, and Akaike infor-
55 mation criteria, were used to evaluate the models' performance.

56 Results

57 Significantly different GABA+ and GABA estimates were found when a well-parameterized
58 MM_{3co} basis function was included in the model. The mean GABA estimates were significantly
59 lower when modeling MM, while the CVs were similar. A sparser spline knot spacing led to
60 lower variation in the GABA and GABA+ estimates, and a narrower modeling range – only in-
61 cluding the signals of interest – did not substantially improve or degrade modeling performance.
62 Additionally, results suggest that LCM can separate GABA and the underlying co-edited MM_{3co} .
63 Incorporating homocarnosine into the modeling did not significantly improve variance in
64 GABA+ estimates.

65

66 Conclusion

67 GABA-edited MRS is most appropriately quantified by LCM with a well-parameterized co-
68 edited MM_{3co} basis function with a constraint to the non-overlapped $MM_{0,93}$, in combination with
69 a sparse spline knot spacing (0.55 ppm) and a modeling range between 0.5 and 4 ppm.

70 **Introduction**

71 A recent expert consensus paper recommended that linear combination modeling (LCM) should
72 be used for the quantification of edited MRS data¹, stating that standard fitting approaches origi-
73 nally optimized for short-TE MRS should be adapted for edited MRS. Further, it was recom-
74 mended that quantum-mechanical simulations should be used to confirm the co-edited profile of
75 all metabolites in the edited spectrum, and contributions from macromolecule (MM) signals
76 should be specified. Despite these recommendations, little detail was given regarding several
77 unique features of edited spectra, and how they should be appropriately modeled. These features
78 include:

- 79
- 80 1) The MEGA-PRESS experiment is well-known to co-edit MM signals with coupled spins
81 at 1.7 and 3 ppm, causing substantial contamination of the edited GABA signal, and
82 forcing researchers to report the composite measure GABA+MM (GABA+)¹. Because
83 the co-edited MM signal is poorly characterized, there is currently no consensus or
84 recommendation on how to appropriately account for it during spectral modeling.
85 Instead, the most widely used analysis algorithms implement entirely different strategies
86 to fit the composite 3-ppm signal. For example, the Gannet software uses a single
87 Gaussian model², while a double-Gaussian is used in Tarquin³, and LCMoel⁴ defaults to
88 a basis set that only includes the GABA basis function.
 - 89 2) Another co-edited compound contributing to the 3 ppm signal is homocarnosine (HCar),
90 a dipeptide of GABA and histidine. While the 3 ppm multiplets of GABA and
91 homocarnosine are separated by just 0.05 ppm (which are therefore unlikely to be
92 successfully separated), inclusion of a homocarnosine basis function may be warranted
93 based on its reported concentration in vivo (~0.5 mmol/kg⁵, compared to ~1-2 mmol/kg
94 for GABA), but it has not been investigated whether doing so has a stabilizing or
95 destabilizing effect on the modeling⁶.
 - 96 3) Unedited spectra are typically modeled over a restricted frequency-domain range
97 covering the visible upfield peaks, including macromolecular and lipid resonances
98 between 0 and 1 ppm, but usually avoiding the water suppression window above ~4 ppm.
99 The choice of frequency-domain modeling range for edited spectra is less obvious. Since

100 the main advantage of spectral editing is the isolation of a single target resonance,
101 modeling signals outside the immediate surrounding of the target may dilute the resolving
102 power of editing. On the other hand, increasing the modeling range may offer useful
103 constraints to stabilize the solution of the modeling problem. The difference is
104 highlighted by the different strategies encountered in common software tools – while the
105 Gannet software fits the GABA-edited difference spectrum over a narrow range (only
106 including the 3-ppm GABA+ and 3.75 ppm glutamate and glutamine peaks), the
107 LCMModel recommendation is to include the strong co-edited signals from glutamate
108 (Glu), glutamine (Gln), glutathione (GSH), N-acetylaspartylglutamate (NAAG), and N-
109 acetylaspartate (NAA), which heavily overlap with GABA around 2.25 ppm. The effects
110 of limiting the modeling range have not been assessed systematically to date.

111 4) Linear combination modeling methods commonly include terms to account for smooth
112 baseline curvature, usually parametrized from cubic B-spline or polynomial functions, or
113 by smoothing residuals. The flexibility of the baseline model substantially affects
114 metabolite estimates from unedited spectra⁷; while baseline terms are necessary to
115 account for e.g. lipid contamination, poor water suppression etc., they are potential
116 sources of overfitting if awarded too many degrees of freedom. Baseline modeling may
117 have an even greater influence when modeling difference spectra, since only *co-edited*
118 lipid and MM signals contribute to the smooth background variation. Importantly, the co-
119 edited MM background of the GABA-edited difference spectrum has not been
120 appropriately characterized (e.g., through metabolite-nulled acquisition), suggesting that
121 the choice of baseline flexibility can drastically influence modeling results through two
122 highly susceptible regions of the spectrum. First, in the absence of an appropriate model
123 for the co-edited broad MM signal at 3 ppm, this signal may be absorbed into the baseline
124 depending on its flexibility. Second, strong MM and lipid signals in the region between
125 0.5 and 2.5 ppm may be affected by the 1.9 ppm editing pulse (either directly through
126 saturation or indirectly through coupling), likely leading to an unknown, but substantial,
127 MM contribution in this spectral region^{8,9}. This is especially important considering that
128 the co-edited signals from NAA, NAAG, Glu, Gln, and GSH overlap with GABA in this
129 region. Overly rigid baselines may provide insufficient flexibility to capture these signals,
130 in turn compromising the accuracy of the estimation of the co-edited metabolites.

131 The aim of this study was to evaluate different strategies for linear combination modeling of
132 GABA-edited MEGA-PRESS difference spectra, and to establish initial ‘best practices’ substan-
133 tiating the recommendations of the expert consensus on spectral editing. To this end, different
134 approaches to account for co-edited MM signals, various modeling ranges and baseline knot
135 spacings, as well as the inclusion of homocarnosine were compared. In the absence of a ‘gold
136 standard’, the performance of each modeling strategy was assessed by comparing descriptive sta-
137 tistics of the metabolite estimates, calculating the Akaike information criteria, and assessing the
138 fit residuals.

139 **Methods**

140 Study participants & data acquisition

141 In this study, 61 publicly available GABA-edited MEGA-PRESS datasets originating from 7
142 sites from a recent 3T multi-center study¹⁰ were analyzed (see **Supplementary Material 1** for
143 subject list). All datasets were acquired on Philips 3T scanners with the following acquisition
144 parameters: TR/TE = 2000/68 ms; 320 excitations (10m 40s scan time); 16-step phase-cycle; 2
145 kHz spectral width; 2000 samples; 27-ml cubic voxel volume in the medial parietal lobe. For this
146 heuristic approach of exploring the GABA modeling, the data homogeneity (SNR, FWHM, tis-
147 sue composition, and absence of fat contamination) was increased while reducing the overall
148 number of subjects by including only 61/298 subjects of the original dataset¹⁰. All sites except
149 for P8 used a similar sequence implementation with interleaved water referencing for prospective
150 frequency correction¹¹. For the edit-ON transients, the editing pulses with 15 ms pulse duration
151 and 82.5 Hz inversion bandwidth (FHWM) were applied at a frequency of 1.9 ppm to refocus the
152 coupling evolution of the GABA spin system. For the edit-OFF transients, the editing pulses
153 were applied at a frequency of 7.5 ppm. Edit-ON and edit-OFF transients were acquired in alter-
154 nating order. An additional water reference scan was acquired for each dataset using interleaved
155 water referencing¹¹, i.e. one excitation with water suppression and editing pulses deactivated
156 every 40 water-suppressed excitations (total of 8 averages).

157

158 Data pre-processing

159 Data were analyzed in MATLAB using Osprey^{12,13} (v.1.0.1.1), a recently published open-source
160 MRS analysis toolbox. Raw data were eddy-current-corrected¹⁴ based on the water reference,
161 and individual transients were aligned separately within the edit-ON and edit-OFF conditions
162 using the robust spectral registration algorithm¹⁵. Averaged edit-ON and edit-OFF spectra were
163 aligned by optimizing relative frequency and phase such that the water signal in the difference
164 spectrum was minimized. The final difference spectra for quantification were generated by sub-
165 tracting the edit-OFF from the edit-ON spectra. Finally, any residual water signal was removed
166 with a Hankel singular value decomposition (HSVD) filter¹⁶ to improve data quality in the edit-
167 OFF spectra and to reduce residual baseline roll in the difference spectra.

168

169 Basis set

170 The basis set used for modeling was generated from a fully localized 2D density-matrix simula-
171 tion of a 101 x 101 spatial grid (voxel size: 30 mm x 30 mm x 30 mm; field of view: 45 mm x 45
172 mm x 45 mm) implemented in a MATLAB based simulation toolbox FID-A¹⁷, using vendor-
173 specific refocusing pulse shape and duration, sequence timings, and phase cycling. It contains 17
174 metabolite basis functions (ascorbate, aspartate, creatine (Cr), negative creatine methylene (-
175 CrCH₂), GABA, glycerophosphocholine, GSH, Gln, Glu, water, myo-inositol, lactate, NAA,
176 NAAG, phosphocholine, phosphocreatine (PCr), phosphoethanolamine, scyllo-inositol, and
177 taurine) and 8 Gaussian MM and lipid resonances (MM_{0.94}, MM_{1.22}, MM_{1.43}, MM_{1.70}, MM_{2.05},
178 Lip09, Lip13, Lip20, details in **Supplementary Material 2** with similarly defined
179 parametrization as described in the LCMoel software manual¹⁸) for the edit-OFF spectrum.

180
181 For the difference spectrum, MM_{0.94} and the co-edited macromolecular signal at 3 ppm (MM_{3co})
182 were parametrized as Gaussian basis functions (MM_{0.94}: 3-proton signal; chemical shift 0.915
183 ppm, full-width at half-maximum (FWHM) 11 Hz; MM_{3co}: 2-proton signal; chemical shift 3
184 ppm; FWHM 14 Hz). The MM_{3co} amplitude was defined under the assumptions of a pseudo-
185 doublet GABA signal at 3 ppm and the MM_{3co} contribution to the 3-ppm GABA peak to be
186 around 50%^{1,6,8,19}. The optimum FWHM used to parametrize the MM_{3co} basis function was de-
187 termined to be 14 Hz by fitting the mean difference spectrum of all datasets with a composite
188 GABA+ basis function (GABA + MM_{3co}) with varying FWHM (between 1 and 20 Hz). The pa-
189 rameterized Gaussian MM_{3co} basis function was integrated into the modeling process using dif-
190 ferent assumptions and constraints described in the following paragraphs.

191

192 Linear combination modeling of GABA-edited difference spectra

193

194 Osprey's frequency-domain linear combination model was used to determine the metabolite es-
195 timates. Model parameters include metabolite basis function amplitudes, frequency shifts, ze-
196 ro/first order phase correction, Gaussian and Lorentzian linebroadening, and cubic spline base-
197 line coefficients. All parameters are determined by Levenberg-Marquardt^{20,21} non-linear least-
198 squares optimization, using a non-negative least-squares (NNLS) fit²²⁻²⁴ to determine the me-
199 tabolite amplitudes and baseline coefficients at each iteration of the non-linear optimization.

200 Amplitude ratio soft constraints are imposed on MM and lipid amplitudes, as well as selected
 201 pairs of metabolite amplitudes, as defined in the LCMModel manual^{4,18}. The strength factor of the
 202 amplitude ratio soft constraint λ is set to 0.05 by default.

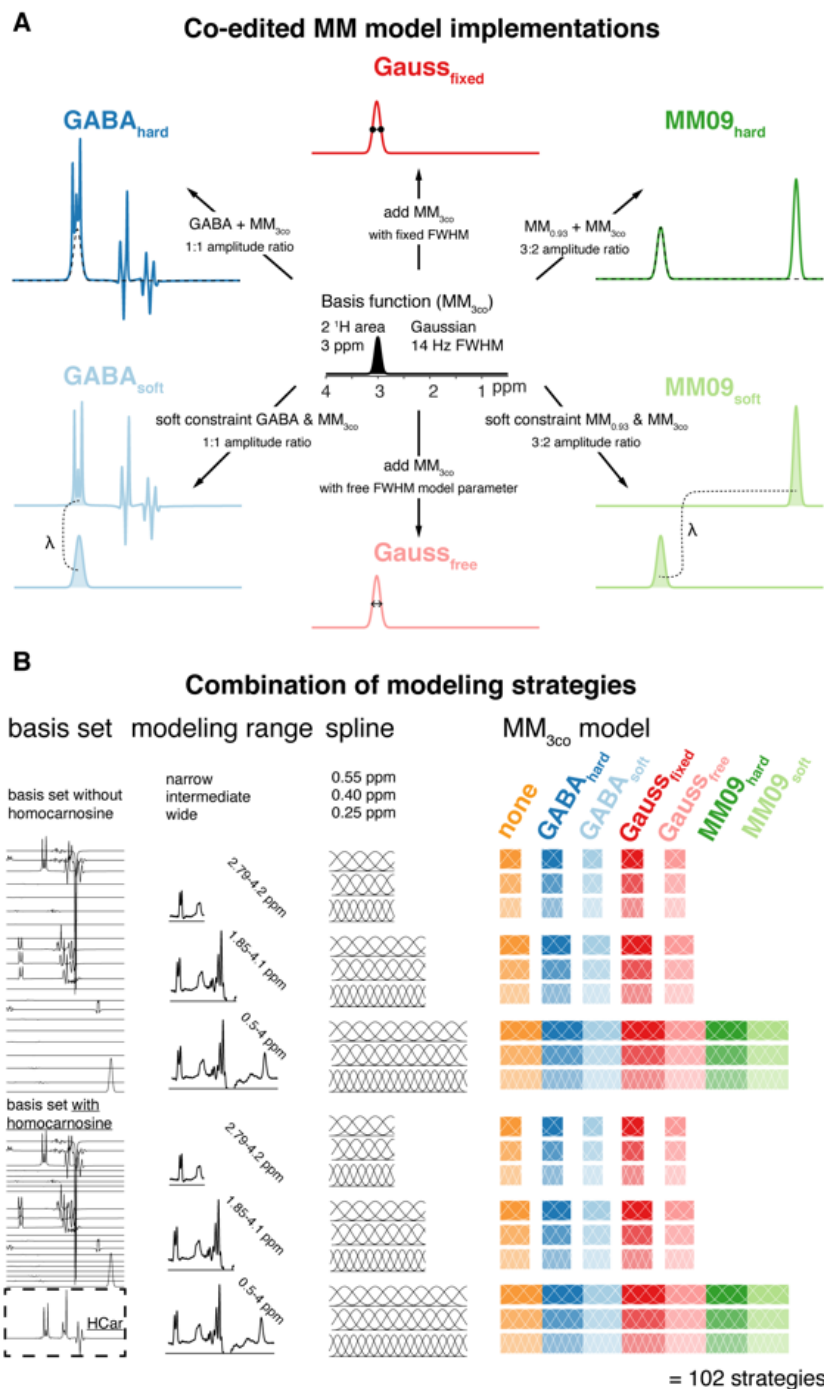


Figure 1 – Different linear combination modeling strategies for GABA-edited spectra. (A) Different co-edited MM₃₀₀ modeling approaches derived from a Gaussian function at 3.0 ppm (B)

All combinations of basis set composition, modeling range, spline knot spacing, and MM_{3co} modeling leading to 102 different modeling strategies.

203 A range of modeling strategies for the GABA-edited difference spectrum was included in this
204 study, covering various aspects of the modeling process (**Figure 1**). The different
205 parametrizations and soft constraints to account for the co-edited MM_{3co} signal are shown in
206 **Figure 1A**. All possible combinations for the modeling strategies: i) inclusion of homocarnosine
207 in the basis set; ii) different modeling ranges; iii) different baseline spline knot spacings and iv)
208 different parametrizations and soft constraints to account for the co-edited MM_{3co} signal are
209 tabulated graphically in **Figure 1 B**. Each modeling aspect is described in detail below:

210

211 *Including homocarnosine in the basis set*

212 To assess the effects of including homocarnosine in the linear combination model, we repeated
213 all analysis steps with two different basis sets: the default Osprey basis set *with* and *without* an
214 additional HCar basis function. Chemical shift and scalar coupling parameters describing the
215 HCar spin system were taken from literature⁶.

216

217 *Varying the modeling range and baseline knot spacing*

218 Two aspects of linear combination modeling are suggested to have a considerable influence on
219 metabolite estimates^{7,25}. First, the choice of the modeling range, i.e., the frequency interval that
220 defines the part of the frequency-domain spectrum that is considered to calculate the least-
221 squares difference between model and data. Second, the baseline knot spacing, i.e., the frequency
222 difference between two adjacent knots of the cubic spline basis that is used to approximate the
223 smooth baseline.

224

225 Three different modeling range scenarios were considered, reflecting common choices in the lit-
226 erature and widely used software tools: a) a wide modeling range typically used to analyze uned-
227 ited spectra, including all signals in the GABA-edited difference spectrum (0.5 to 4 ppm –
228 “*wide*”); b) an intermediate modeling range excluding signals below 1.9 ppm (e.g. co-edited li-
229 pids and macromolecules), but including strong co-edited signals from NAA, NAAG, Glu, Gln,
230 and GSH (1.85 and 4.1 ppm, “*intermediate*”), similar to the range recommended in LCMoDel’s
231 dedicated ‘mega-press-3’ option; and c) a narrow modeling range only including the co-edited

232 signals from GABA+ and Glx (2.79 – 4.2 ppm, "narrow"), the default modeling range in Gan-
233 net².

234

235 Three spline knot spacings were included in the analysis, with 0.4 ppm being the default Osprey
236 option, shown to create reproducible and comparable metabolite estimates for conventional MRS
237 ²⁶, as well as sparser (0.55 ppm) and denser (0.25 ppm) spline knot spacings.

238

239

240 Co-edited macromolecule models

241 Seven different strategies to model the GABA-edited difference spectrum were implemented
242 (**Figure 1 A**). The trivial approach – not accounting for the co-edited signal MM_{3co} at all – is la-
243 beled **none**. The other six modeling strategies all include a dedicated parametrized Gaussian
244 MM_{3co} basis function. This basis function is given different degrees of freedom in the different
245 strategies, e.g., hard- or soft-constrained relative to the amplitude of the GABA or the MM_{0,94}
246 basis functions, and with a fixed or free width. Here, strategies with fewer degrees of freedom
247 reflect the frequently made assumption that the GABA-to-MM ratio (and the MM background
248 itself) is relatively stable across subjects and anatomical region, and assumed to be known, while
249 strategies with more degrees of freedom or soft constraints relax these assumptions:

- 250 • The **GABA_{hard}** model uses a single composite GABA+MM basis function by adding the
251 GABA and MM_{3co} (initial FWHM of the basis function = 14 Hz) basis functions with a fixed
252 1:1 amplitude ratio. The 1:1 ratio reflects the widely used empirical assumption that 50% of
253 the 3-ppm signal in a conventional GABA-edited difference spectrum can be attributed to co-
254 edited macromolecules^{6,19}.
- 255 • The **GABA_{soft}** model uses separate GABA and MM_{3co} (initial FWHM of the basis function =
256 14 Hz) basis functions and imposes a soft constraint on the ration of the amplitudes of both
257 basis functions during the optimization (1:1 ratio).
- 258 • The **Gauss_{fixed}** model uses separate GABA and MM_{3co} (initial FWHM of the basis function =
259 14 Hz) basis functions. No further constraints are imposed. This means possible changes in
260 the contributions to the 3-ppm GABA peak are modeled.
- 261 • The **Gauss_{free}** model uses separate GABA and MM_{3co} basis functions. In contrast to the
262 Gauss_{fixed} model, the FWHM of the Gaussian MM_{3co} signal is represented by an additional

263 model parameter. This means that the MM_{3co} basis function itself is not static, but
264 dynamically modified during optimization.

- 265 • The $MM09_{hard}$ model uses separate GABA and MM basis functions. The MM_{3co} basis
266 function is replaced by a composite $MM_{0,94} + MM_{3co}$ basis function (i.e., the $MM_{0,94}$ (initial
267 FWHM of the basis function = 11 Hz) and MM_{3co} (initial FWHM of the basis function = 14
268 Hz) basis functions are added in a 3:2 ratio). The result is a single composite basis function
269 for $MM_{0,94}$ and MM_{3co} , adapted from the soft constraint model described in the literature⁹.
- 270 • The $MM09_{soft}$ model uses separate GABA, $MM_{0,94}$ and MM_{3co} basis functions. In contrast to
271 the $MM09_{hard}$ model, soft constraints enforce a ~3:2 amplitude ratio for the $MM_{0,94}$ and
272 MM_{3co} amplitudes during optimization. The use of two separate but linked basis functions for
273 $MM_{0,94}$ and MM_{3co} is similar to previously described implementations⁹.

274 The models $MM09_{hard}$ and $MM09_{soft}$ ²⁷ as well as $Gauss_{fixed}$ ²⁸ correspond to models previously
275 investigated using the LCMModel software and the amplitude assumptions were derived empirical-
276 ly. It is worth repeating here, that each basis function receives a separate Lorentzian
277 linebroadening, frequency shift, and amplitude parameter during the optimization, in addition to
278 the global parameters (zero/first order phase correction, global frequency shift, and Gaussian
279 linebroadening). For the $Gauss_{free}$ model, the MM_{3co} basis function is dynamically updated as an
280 explicit modeling parameter during the optimization, therefore the MM_{3co} basis function has ef-
281 fectively two separate adjustable parameters to account for its linewidth (the Lorentzian
282 linebroadening term and the FWHM of the MM_{3co} basis function). Finally, the composite models
283 $GABA_{hard}$ that lacks separate GABA and MM functions has only one linebroadening, one fre-
284 quency, and one amplitude parameter compared to twice the parameters for its soft constraint
285 counterparts.

286
287 Combining the various MM_{3co} models (5 + 2 that were used for the wide modeling range only),
288 modeling ranges (3), baseline spline knot spacings (3), and basis sets (2), a total of 102 different
289 modeling strategies were investigated in this study. All models were implemented in Osprey¹²
290 and are available on GitHub¹³.

291

292 Quantification, visualization, and statistics

293 Quantification

294 For the basis set without homocarnosine, GABA refers to the model amplitude estimate for the
295 GABA basis function, which is of course only available for the modeling strategies with separate
296 basis functions for GABA and MM_{3co} (none, GABA_{soft}, Gauss_{fixed}, Gauss_{free}, MM09_{soft}). GABA+
297 refers to the sum of the amplitude estimates for GABA and MM_{3co} (GABA_{soft}, Gauss_{fixed},
298 Gauss_{free}, MM09_{hard}, MM09_{soft}) or the amplitude estimate for the composite basis function in-
299 cluding both MM and GABA (GABA_{hard}) and is therefore calculated for all strategies with an
300 explicit MM_{3co} model. For comparison, the GABA amplitude for the `none` strategy is included
301 in the figures reporting GABA + MM_{3co}. However, it still refers to a GABA-only estimate.
302 For the basis set that included homocarnosine (HCar), the difference in GABA and MM_{3co} esti-
303 mates between the modeling strategies with and without HCar (Δ GABA and Δ MM_{3co}, respec-
304 tively) were investigated to evaluate whether the inclusion of HCar has a systematic effect on the
305 estimation of those signals with which it overlaps. All estimates were quantified relative to the
306 total creatine (Cr + PCr) amplitude from the edit-OFF spectrum with the wide modeling range
307 and a spline knot spacing of 0.4 ppm. Differences in GABA(+)/tCr between modeling strategies
308 are therefore only related to the modeling of the difference spectra, but not to the reference com-
309 pound modeling. No further tissue or relaxation corrections were applied.
310 Further, the relative contributions of MM_{3co} to the GABA+ estimate and the relative contribu-
311 tions of HCar to the sum of GABA+ and HCar estimate were calculated.

312

313 Visualization

314 The modeling performance and systematic characteristics of each modeling strategy were visual-
315 ly assessed through the mean spectra, mean fit, mean residual, and mean models of GABA+,
316 GABA, MM_{3co}, HCar (if included) and the baseline, i.e., averaged across all datasets.

317

318 The metabolite estimate distributions were visualized as violin plots including boxplots with me-
319 dian, 25th/75th quartile ranges, and smoothed distributions to identify systematic differences be-
320 tween modeling strategies. In addition, the mean value of the `none` model across the three
321 spline knot spacings was added for each modeling range as a dashed horizontal line. Bar plots

322 were created to visualize quality metrics, including the standard deviation if appropriate. All
323 plots were generated with R²⁹ (Version 3.6.1) in RStudio (Version 1.2.5019, RStudio Inc.) using
324 SpecVis^{26,30}, an open-source package to visualize linear combination modeling results with the
325 ggplot2 package³¹. All scripts and results are publicly available³².

326

327 Statistics

328 Significant differences in the mean and the variance of the GABA, GABA+, and MM_{3co} esti-
329 mates were assessed between all modeling strategies. The statistical tests were set up as paired
330 without any further inference. Differences of variances were tested with Fligner-Killeen's test,
331 with a post-hoc pair-wise Bonferroni-corrected Fligner-Killeen's test. The means were compared
332 with an ANOVA or a Welch's ANOVA, depending on whether variances were different or not.
333 Post-hoc analysis was performed with a paired t-test with equal or non-equal variances, respec-
334 tively.

335

336 Additionally, Pearson's correlation was used to investigate the impact of including HCar in the
337 basis set. The strength of the correlation was considered substantial for $R > 0.25$.

338 Model evaluation criteria

339 The performance of each modeling strategy was evaluated in different ways, including the im-
340 pact of the different modeling strategies on the GABA, GABA+ , and MM_{3co} estimates, as well
341 as several quality measures:

- 342 1) Visual inspection: Mean model, residual, and baseline were assessed for characteristic
343 features.
- 344 2) SD fit quality: The SD of the residual was determined, and then normalized by the noise
345 level (calculated as the SD of the noise between -2 and 0 ppm). This was done over the
346 entire modeling range of the difference spectrum and termed **residual_{SD} range**.
- 347 3) Amplitude fit quality: the difference between the maximum and minimum of the residual
348 was determined, and then normalized by the noise level²⁵ (similarly calculated as in the
349 second criterion). This was done over the entire modeling range of the difference
350 spectrum and termed **residual_{ampl} range**.

- 351 4) Amplitude 3-ppm peak fit quality: Similar to the third criterion, the residual was
352 calculated over the range of 3.027 ± 0.15 ppm to assess the fit quality of the 3-ppm
353 GABA peak and termed **residual_{ampl 3ppm}**.
- 354 5) Consistency of metabolite estimates: The across-subject coefficients of variation (CV =
355 SD/mean) for all metabolite estimates (GABA/tCr, GABA+/tCr) were calculated for each
356 modeling strategy.
- 357 6) Akaike Information Criterion (AIC): The Akaike information criterion ³³, which takes the
358 number of model parameters into account, is defined as follows:

$$\logLikelihood_i = -0.5 * N_i * (\log(2 * \pi) + 1 - \log(N_i) + \log(SSE_i))$$

359

$$AIC_i = -2 * \frac{1}{N_i} * \logLikelihood_i + 2K_i$$

360 Here, N_i is the number of points in the modeling strategy i , SSE_i is the sum of squared
361 error (i.e., squared residual) of that strategy, and K_i is the number of free model parame-
362 ters for that strategy. The \logLikelihood_i was divided by the number of points N_i to re-
363 duce the strong weighting of the datapoints and to make the AIC_i values comparable for
364 different modeling ranges. Soft constraint model parameters were included with a value
365 of 0.5. Lower AIC_i values indicate a more appropriate model. Subsequently, ΔAIC_i
366 scores were calculated as the difference of AIC_i of modeling strategy i and the model
367 with the lowest AIC_{min} :

$$\Delta AIC_i = AIC_i - AIC_{min}$$

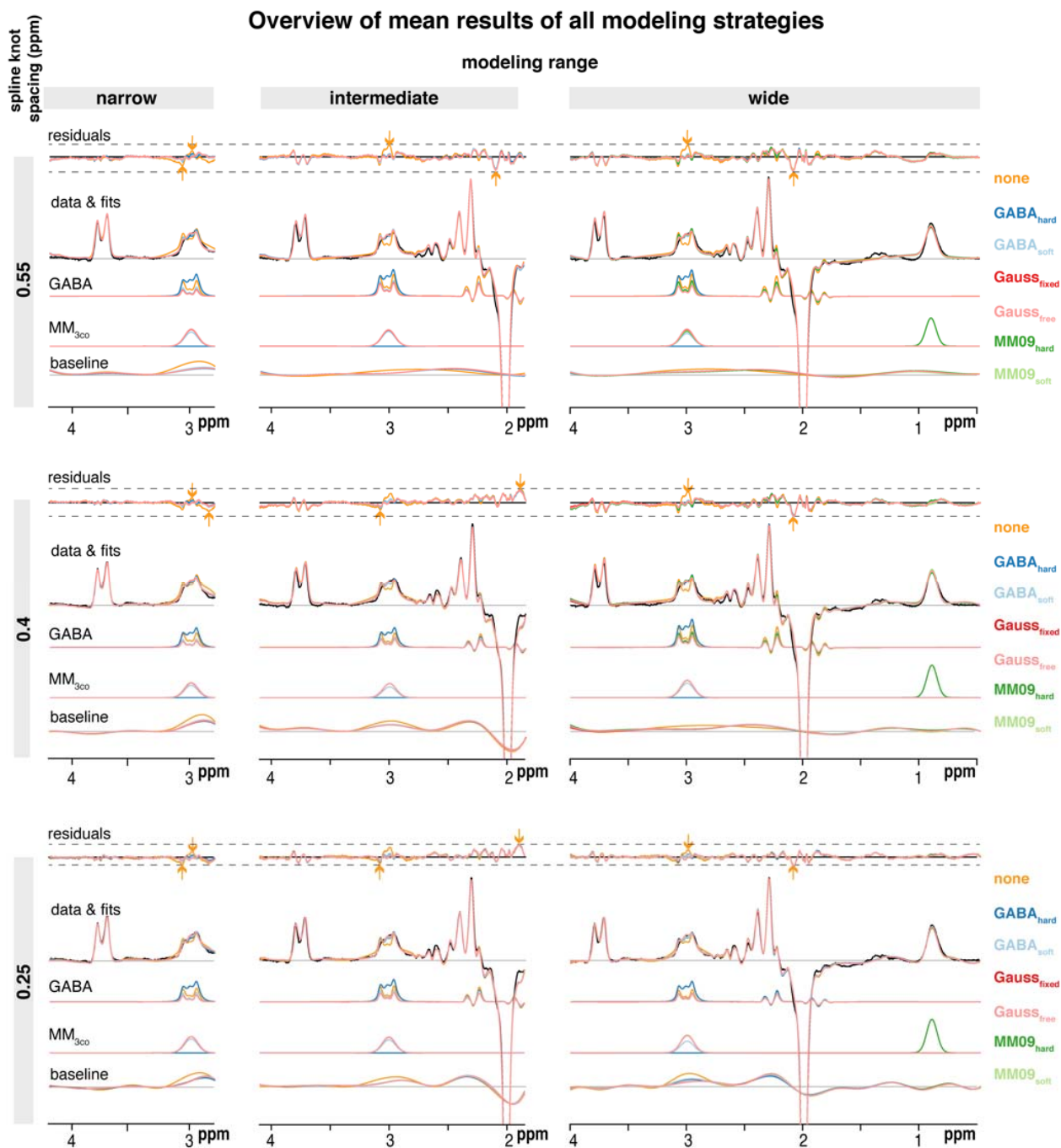
368

369 **Results**

370 All 61 datasets were successfully processed and modeled with all 102 modeling strategies. No
371 data were excluded from further analysis. The data quality assessment indicated consistently
372 high spectral quality for all spectra ($NAA_{SNR} = 272 \pm 70$; $NAA_{FWHM} = 5.29 \pm 1.09$ Hz) without
373 lipid contamination. Individual spectra as well as the mean spectrum and SD are displayed in
374 **Supplementary Material 3**. Other data quality measures were extracted from the Gannet² anal-
375 ysis performed in recent multi-site studies^{10,34}. For the Philips-only subset of datasets in the pre-
376 sent study, the tissue composition ($fGM = 0.60 \pm 0.04$; $fWM = 0.27 \pm 0.03$; $fCSF = 0.13 \pm 0.04$)
377 and across-subject CV ($GABA+/Cr = 9.99\%$) indicate consistency in the dataset and the model-
378 ing. Across-subject CV was interpreted as a measure of modeling performance, assuming that
379 increased CVs are mainly introduced by variability in the modeling and do not reflect biological-
380 ly meaningful variance of GABA+ estimates.

381 **Summary and visual inspection of the modeling results**

382

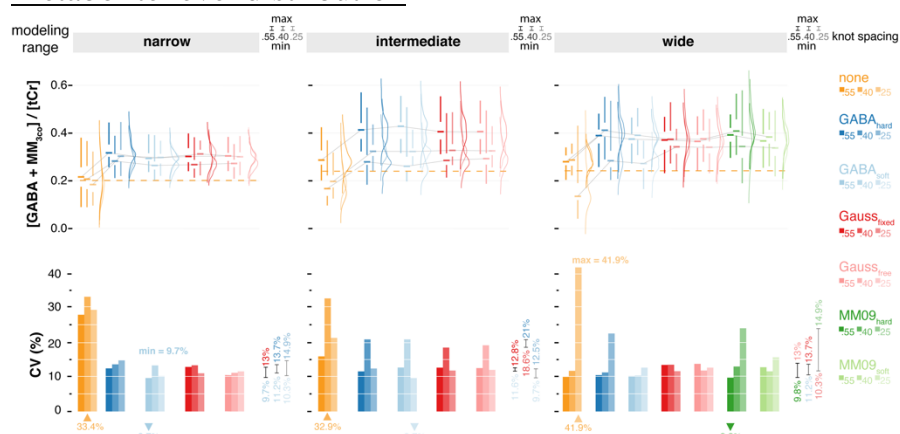


383

Figure 2 – Mean modeling results for all modeling strategies without homocarnosine. A substantial structured residual is apparent at 3 ppm if no MM modeling strategy is included. All three modeling ranges (columns), three spline knot spacings (rows), and MM_{3co} model (color-coded) are presented with mean residuals and fits, as well as the GABA+, GABA, MM_{3co}, and spline baseline models. The mean data is included in black. The dashed lines indicate the range of the residual across one row. The arrows indicate the range of values for a specific modeling range and spline knot spacing with the color corresponding to the MM_{3co} model with minimum/maximum value.

384
385 **Figure 2** shows the mean modeling results for all modeling strategies without homocarnosine.
386 Not including MM_{3co} leads to a substantial structured residual around 3 ppm for all knot spacings
387 and modeling ranges. In contrast, all modeling strategies with MM_{3co} appear to reflect the
388 lineshape of the 3-ppm signal more accurately, with very similar results for the complete fit (me-
389 tabolites, MMs, and baseline) and the individual components. Modeling strategies with the in-
390 termediate and wide modeling range further show strong residuals around 2 ppm, suggesting
391 slightly inaccurate lineshape modeling of the methyl singlets from NAA and NAAG, or inaccu-
392 rate modeling of co-edited MM signals in this region. Structured residuals appear also in the re-
393 gion of the 3.75 ppm Glx signals, although they are much less pronounced in strategies with the
394 narrow modeling range, suggesting that including the 2.25 ppm multiplets (and underlying base-
395 line fluctuation) has a considerable impact on phase estimation.
396 In general, the residuals are consistent between different MM_{3co} models for any given knot spac-
397 ing and modeling range. Notably, residuals tend to be smaller on an absolute scale for denser
398 knot spacing and narrower modeling range.
399 Mean GABA models agree well between all strategies with a separate MM_{3co} model. The
400 $GABA_{hard}$ strategy appears to produce a larger signal as its GABA basis function includes the
401 MM_{3co} signal, but does not model it separately, while the strategies that do so produce compara-
402 ble mean MM_{3co} models.
403 The mean baseline is consistently flatter around 3 ppm for modeling strategies with an explicit
404 MM_{3co} model, while absorbing substantially more signal for the ‘none’ approach without an MM
405 model. This behavior is particularly obvious for the dense knot spacing (0.25 ppm) over the wide
406 modeling range. Baseline curvature generally increases for denser knot spacings around 2.2 ppm
407 for the intermediate and wide range.
408

409 **Metabolite level distribution**



410 **Figure 3 – Distribution and across subject coefficients of variation (CVs) of GABA+ estimates for all modeling strategies. Including a MM_{3co} model significantly increases the mean estimates for all modeling strategies, while giving similar or reduced CVs. The mean estimates across the three spline knot spacings of the ‘none’ approach are indicated as a dashed line for each modeling range. All three modeling ranges (column) and three spline knot spacings (within each column), and co-edited MM models (color-coded) are presented. Distributions are shown as half-violins (smoothed distribution), box plots with median, interquartile range, and 25th/75th quartile. The median lines of the box plots are connected to visualize trends within a specific baseline knot spacing. CVs are summarized as bar plots. Minimum/maximum CVs for each modeling range are indicated as downwards/upwards triangles in the color corresponding to the MM_{3co} model. Minimum/maximum CVs for each baseline knot spacing within a specific modeling range are reported on the right side of each column. Global minimum and maximum CVs across all models are added as text.**

411
 412 **Figure 3** shows distributions and coefficients of variation (CVs) of the GABA+ estimates for all
 413 modeling strategies. Table 1 summarizes the mean and SD GABA/GABA+ estimates as well as
 414 the statistics. GABA+ estimates are significantly higher than GABA-only estimates of the ‘none’
 415 modeling strategy for all modeling ranges and knot spacings, supporting the notion from **Figure**
 416 **2** that not including an MM model leaves a considerable fraction of the edited 3-ppm signal
 417 unmodeled, resulting in substantial residuals or increased baseline amplitude flexion.
 418 Notably, all modeling strategies with MM_{3co} return comparable mean estimates and CVs within
 419 the same knot spacing (see Minimum/Maximum column of **Figure 3**). In addition, sparser knot
 420 spacing leads to lower CVs. The intermediate modeling range does not appear to perform more
 421 consistently than both other modeling ranges.

422

423

424 Model evaluation

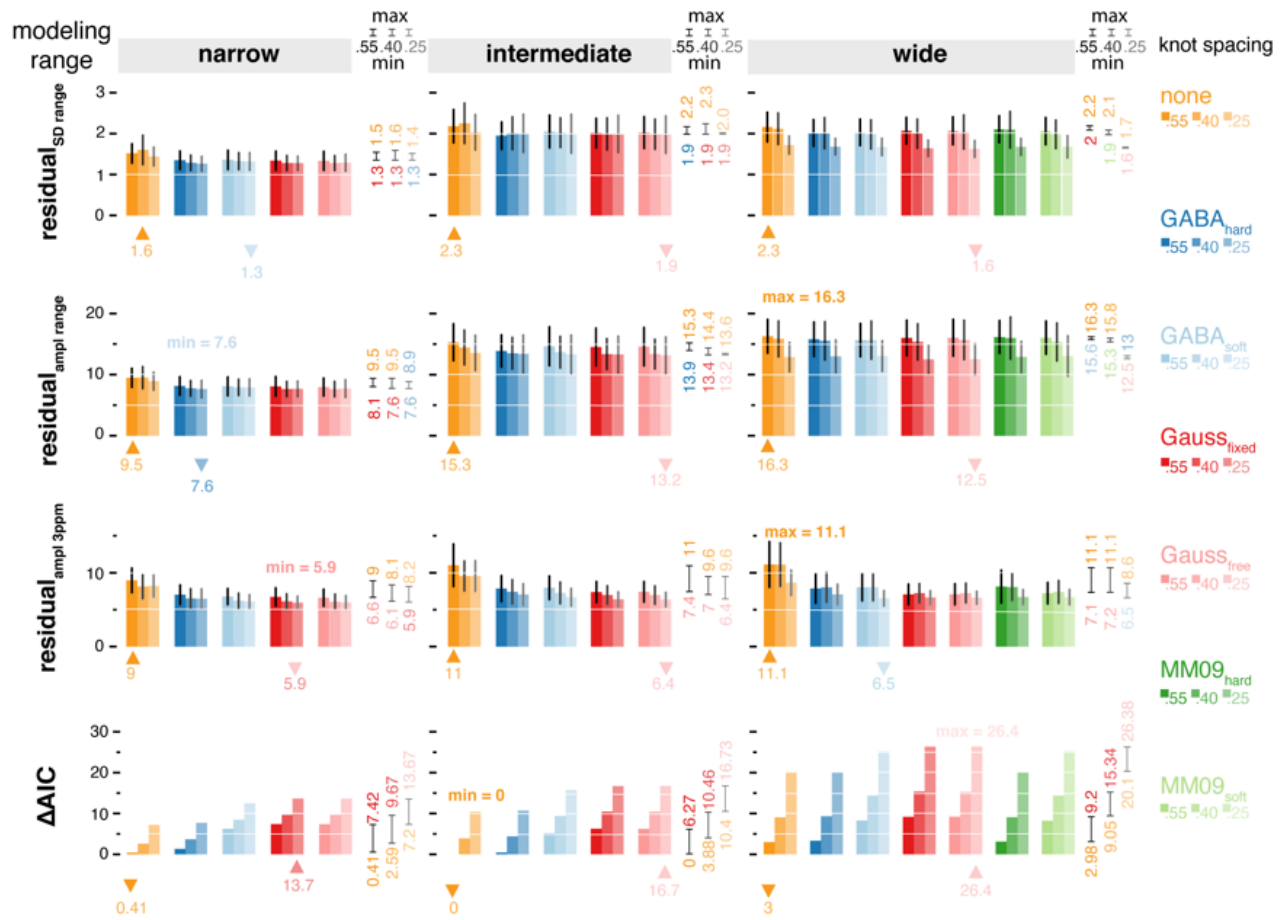


Figure 4 – Evaluation of all modeling strategies. Comparably low residual_{ampl range} are related to the high data quality without artifacts between 0.5 and 2 ppm. Including an MM_{3co} model reduces the 3-ppm residual by ~30% without significant impact on the ΔAIC. All three modeling ranges (column) and three spline knot spacings (within each column), and co-edited MM models (color-coded) are presented. Bar plots represent mean values; SD is indicated by whiskers where appropriate. Minimum/maximum values for each modeling range are indicated as downwards/upwards triangles in the color corresponding to the MM_{3co} model. Minimum/maximum values for each baseline knot spacing within a specific modeling range are reported on the right side of each column. Global minimum and maximum values across all models are added as text.

425 **Figure 4** summarizes the metrics used for model evaluation. The residual over the modeled fre-
 426 quency range (residual_{SD range} and residual_{ampl range}) is lowest for the narrow modeling range. For
 427 the intermediate and wide modeling ranges, residual_{ampl range} is substantially higher, largely driven

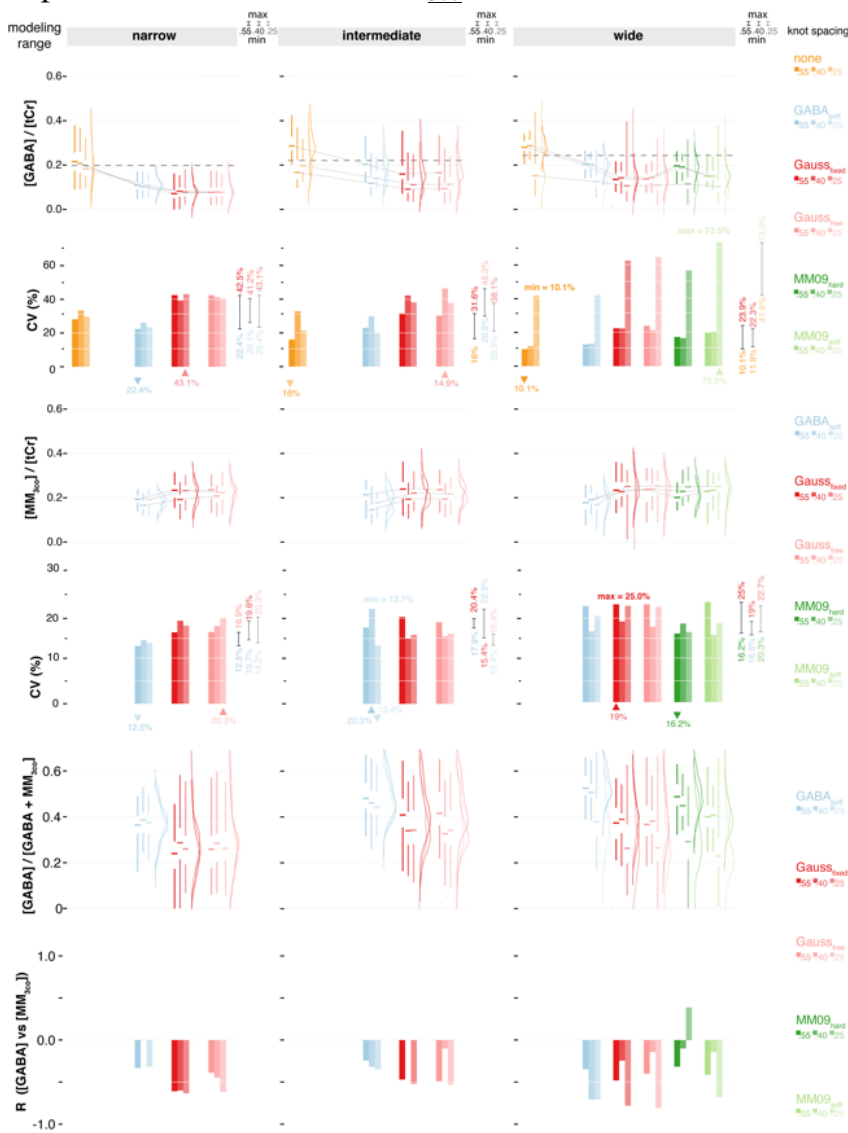
428 by the 2-ppm region (see also **Figure 2**). Consequentially, $\text{residual}_{\text{ampl range}}$ is comparable be-
429 tween MM modeling strategies for a given knot spacing (see Minimum/Maximum column of
430 **Figure 4**).

431 The residual around the GABA⁺ peak ($\text{residual}_{\text{ampl } 3\text{ppm}}$) is consistently reduced by up to 30% if a
432 MM_{3co} model is included, in line with the reduction of structured residual in **Figure 2**. This ef-
433 fect is less pronounced for the dense knot spacing (0.25 ppm), indicating that a flexible baseline
434 is to some degree capable of accounting for otherwise unmodeled MM signal. Together, these
435 findings again support the notion that omitting an explicit MM_{3co} model does not capture the
436 whole edited 3-ppm signal, which remains unmodeled (in the residual) or gets partially absorbed
437 by the baseline or interpreted incorrectly as GABA signal.

438 The strategy with the lowest AIC is the ‘none’ model with the intermediate modeling range and
439 sparse knot spacing, reflecting the low number of model parameters: there is no separate basis
440 function for MM, and the low number of splines. The ΔAIC (the difference between the lowest
441 AIC and the individual model’s AIC) consequently increases for larger modeling ranges, as more
442 splines are included. Similarly, ΔAIC increases for denser knot spacings, and in fact, this in-
443 crease is much stronger compared to the resulting reduction in both residual measures, suggest-
444 ing that the increased flexibility and reduction of the residual does not justify the greater number
445 of model parameters.

446 For any given knot spacing and modeling range, ΔAIC values are comparable between MM_{3co}
447 models, with moderate increases when more parameters are estimated. Together with its low CV
448 (9.8% compared to the minimum CV value 9.7% for the GABA_{soft} value with a narrow fit range)
449 for GABA⁺, the ΔAIC for the MM09_{hard} model over the wide modeling range with sparse knot
450 spacing ($\Delta\text{AIC} = 3.1$) indicates a good performance of this particular model without introducing
451 overfitting. Despite the slightly higher ΔAIC , it is beneficial to opt for the MM09_{hard} model,
452 since the MM_{0.94} peak provides an ‘external’, non-overlapped reference anchor point for the am-
453 plitude of the expected MM₃₀ peak – the MM landscape is thought to be relatively stable across
454 healthy subjects in a narrow age range, at least in the absence of pathology⁸. Furthermore, the
455 MM09_{hard} model does not impose any amplitude assumptions or constraints on the target me-
456 tabolite GABA.

457 Separation of GABA and MM_{3co}



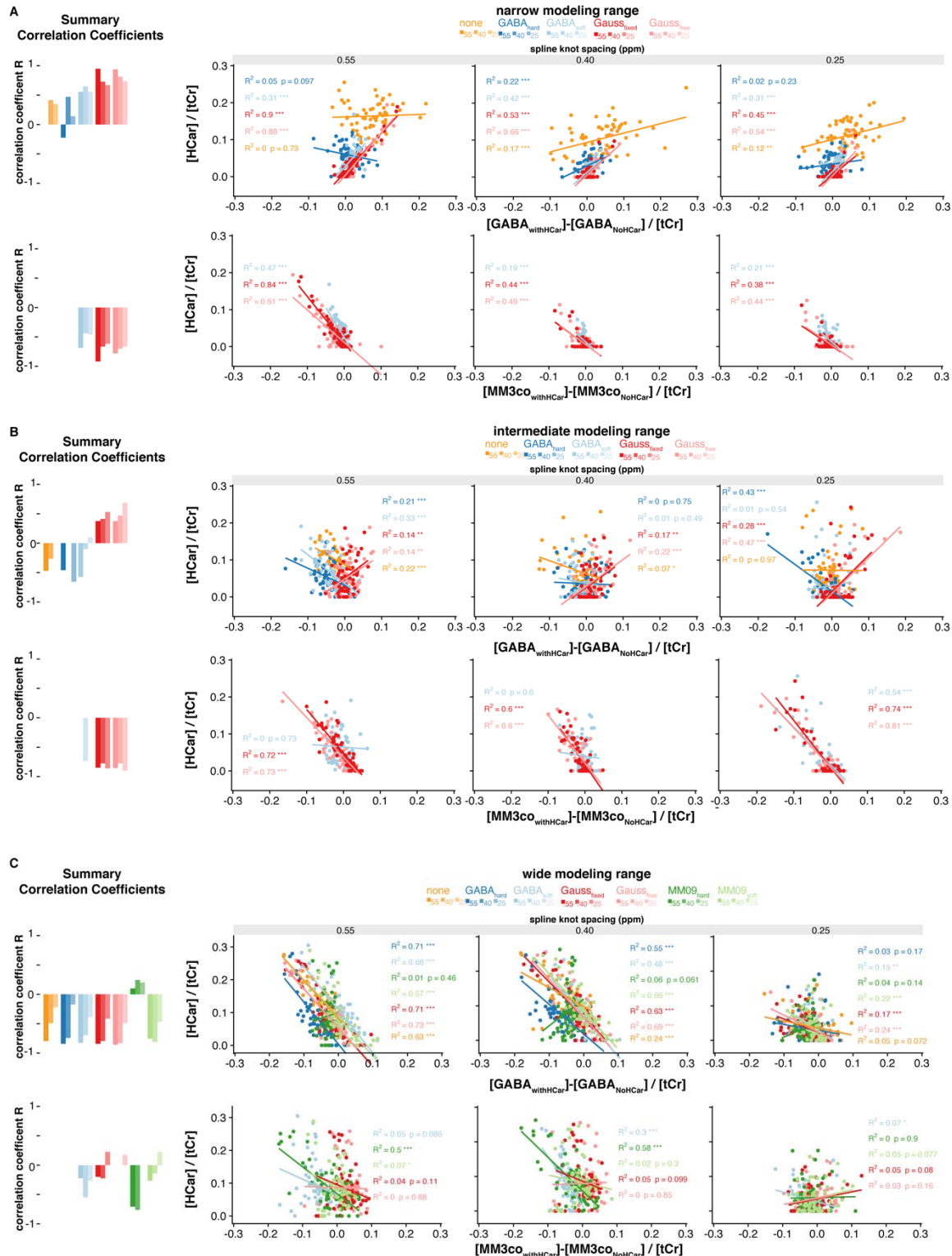
458

Figure 5 - Distribution of GABA and MM_{3co} estimates, relative contribution of GABA to GABA+ and Pearson's R between GABA and MM_{3co} for all modeling strategies. All three modeling ranges (column) and three spline knot spacings (within each column), and MM_{3co} models (color-coded) are presented. Distributions are shown as half-violins (smoothed distribution), box plots with median, interquartile range, and 25th/75th quartile. The median lines of the box plots are connected to visualize trends within a specific baseline knot spacing. The mean estimates across the three spline knot spacings of the 'none' approach are indicated as a dashed line for each modeling range. Across subject CVs are summarized as bar plots. Minimum/maximum CVs for each modeling range are indicated as downwards/upwards triangles in the color corresponding to the MM_{3co} model. Minimum/maximum CVs for each baseline knot spacing within a specific modeling range are reported on the right side of each column. Global minimum and maximum CVs across all models are added as text.

Figure 5 shows the distributions and CVs of the separate GABA and MM_{3co} estimates of all modeling strategies. Including a separate MM_{3co} basis function significantly decreases GABA estimates, suggesting that not doing so may lead to GABA overestimation, as MM signal is mistakenly modeled as GABA. As was seen for the composite GABA+ estimates in **Figure 3**, sparser knot spacing appears to stabilize modeling, leading to lower CVs of GABA. This becomes especially obvious for the wide modeling range, where GABA CVs exceed 50% for dense knot spacing.

MM_{3co} estimates are stable across the different knot spacings, suggesting that the different parametrizations accurately account for most of the co-edited MM signal at 3 ppm.

459 The GABA model, in combination with a wide modeling range and 0.55 ppm knot spacing, ex-
460 hibits the lowest CV for GABA (10.4%). However, the MM09_{hard} model in combination with the
461 same knot spacing and modeling range has only slightly higher GABA CVs (17.3%) with the
462 corresponding MM_{3co} CVs being 16.2% (MM09_{hard}). Again, despite slightly higher CV values it
463 is beneficial to use a modeling strategy with a constraint to an ‘external’ reference peak
464 (MM09_{hard}) instead of the highly overlapped MM_{3co} peak of GABA_{soft} (CV = 12.8%), or entirely
465 omitting MM_{3co}. Additionally, the correlation between the GABA and the MM_{3co} estimates is
466 lower for the MM09_{hard} model, potentially implying a better separation of GABA and MM_{3co}.
467 However, a separation of GABA and co-edited macromolecules remains difficult with a low-to-
468 moderate correlation between GABA and MM_{3co} estimates for all but one modeling strategy
469 (MM09_{hard} for the wide fit range and 0.4 ppm baseline knot spacing). **Supplementary Material**
470 **4** and **5** reports the mean and SDs of the GABA and MM_{3co} estimates as well as the statistics,
471 respectively.
472



473

Figure 6 – Impact of including homocarnosine in the basis set. The directionality of the correlation indicates that HCar absorbs GABA signal specifically for the intermediate and wide modeling range and absorbs MM_{3co} signal for all modeling ranges. Correlation analysis between the differences between GABA/MM_{3co} estimates with and without HCar in the basis set and the

*HCar estimates. All three modeling ranges (A-C) and three spline knot spacings (within each subplot) were investigated. A summary bar plot with the correlation coefficient R is shown in the beginning of each row. Pearson's correlation was calculated for each MM_{3co} model (color-coded). Asterisks indicate significant correlations with $p < 0.05 = *$, $p < 0.01 = **$, and $p < 0.001 = ***$.*

474 Finally, **Figure 6** shows the impact of including HCar into the basis set with the difference in
475 GABA and MM_{3co} estimates between the modeling strategies with and without HCar ($\Delta GABA$
476 and ΔMM_{3co} , respectively). Interestingly, clear differences in the systematic effects of HCar are
477 evident between the modeling ranges:

478 For the narrow modeling range (**Figure 6 A**), HCar estimates correlate positively with $\Delta GABA$,
479 but the correlation is *only* substantial ($R > 0.25$) for strategies with a *separate* MM basis
480 function. For precisely these strategies, HCar estimates correlate negatively with ΔMM_{3co} . These
481 observations suggest that HCar is likely to account for MM_{3co} in the narrow modeling range. In
482 contrast, HCar and $\Delta GABA$ correlate negatively for most strategies in the intermediate and wide
483 modeling ranges (**Figure 6 B** and **C**). The negative correlations between HCar and ΔMM_{3co} are
484 notably weaker for these modeling ranges, indicating that HCar is more likely to substitute for
485 GABA signal instead of MM.

486 This behavior can possibly be explained by the HCar signal shape for each modeling range
487 (**Supplementary Material 6**). For the narrow modeling range, the HCar basis function offers the
488 model an additional degree of freedom to account for deviations of the actual edited 3-ppm
489 signal from pure GABA and the symmetric Gaussian MM_{3co} component, as no resonances
490 below 2.78 ppm are considered. As a result, HCar shows a high correlation with the difference in
491 MM_{3co} . For the intermediate and wide range, the HCar difference spectrum basis function more
492 nearly resembles its GABA counterpart since other resonances are included, thereby more
493 effectively coupling GABA and HCar estimates to each other. Perhaps unsurprisingly, HCar
494 estimates are significantly higher for 'none' modeling strategy, and are substantially lower for
495 more flexible baselines, supporting the notion that HCar rather serves as a substitute for an
496 explicit MM signal, in particular if the baseline cannot absorb the latter (**Supplementary**
497 **Material 6**). Within a given knot spacing and modeling range, HCar estimates are comparable
498 between different MM_{3co} models, a behavior observed for GABA estimates as well.

499 The GABA+ plus homocarnosine estimates show a slight increase compared to the GABA+
500 estimates without HCar (**Supplementary Material 7**). For the 'none' model, stronger changes

501 occur as HCar accounts for MM signal (see also Figure 6). There was no improvement in the
502 CVs observed when including HCar in the model. The relative contribution of HCar to GABA+
503 ranged between 2.2% and 19.1% for modeling strategies with an MM_{3co} basis function and
504 between 18% and 36% for the ‘none’ model.

505

506 **Discussion**

507 The application of linear combination modeling to edited difference spectra is neither straight-
508 forward nor intuitive. The conceptual advantage of spectral editing arises from isolating a re-
509 solved target resonance, i.e. reducing the overlap of the target metabolite with other signals, as
510 well as the number of signals in the spectrum in general¹. LCM, on the other hand, benefits from
511 maximizing the use of prior knowledge to solve the spectral modeling problem, i.e., using all
512 available information for meaningful constraint, including from overlapping signals. The specific
513 case of GABA-edited MRS at 3T poses unique and unresolved challenges. Firstly, a compromise
514 must be drawn between maximizing the prior knowledge by increasing the modeling range and
515 reducing the impact of co-edited and unwanted signals. Secondly, an appropriate parametrization
516 of poorly characterized co-edited signals must be found, and possible interactions with the target
517 metabolite GABA must be evaluated. Thirdly, effects of baseline modeling must be studied,
518 again a consequence of the macromolecular background signal in the GABA-edited difference
519 spectrum not being determined to this date. In this study, a total of 102 linear combination mod-
520 eling strategies were compared for GABA-edited difference spectra, each with different model-
521 ing ranges, parametrizations of co-edited signals, and baseline model flexibility. The key find-
522 ings are:

- 523 • Including a dedicated basis function for co-edited MM improves fit residuals,
524 reduces CVs of GABA and GABA+ estimates, and avoids overestimation of
525 GABA.
- 526 • Reducing the modeling range does not substantially stabilize or destabilize
527 modeling, while removing potentially valuable information (MM_{0.93} and 2-ppm
528 NAA peak) from the optimization.
- 529 • Sparser baseline spline knot spacing leads, on average, to the lowest CV across all
530 modeling ranges.

531 There is surprisingly little systematic investigation into linear combination modeling of GABA-
532 edited difference spectra. To the best of our knowledge, there is only one conference abstract
533 studying MM parametrization in GABA-edited MRS with the LCMModel software²⁷. The results
534 from this preliminary investigation indicate that including a specific MM basis function signifi-

535 cantly reduces GABA estimates, as was also observed in an earlier study²⁸ and which is substan-
536 tiated by our findings.

537

538 Although the substantial contribution of broad MM signals to the 3-ppm peak in the GABA-
539 edited spectrum is widely known^{1,35}, it is rarely explicitly addressed in linear combination mod-
540 eling. Instead, it is assumed that either an incomplete model (without explicit MM term) will still
541 provide an accurate GABA estimate, or that baseline modeling will account for the MM signal.
542 The current results provide evidence that including an appropriately parametrized MM model is
543 a preferable and easily implemented strategy, reducing the residual over the 3-ppm signal range
544 by up to 30%, with similar or lower CVs for GABA+. In contrast, not including an MM model
545 likely causes systematic overestimation of GABA, as the least-squares optimization attempts to
546 minimize the model-data difference with an inadequate set of basis functions (only GABA), par-
547 ticularly when a rigid baseline is chosen. Including MM_{3co} is a justified and reasonable measure
548 without overfitting (reflected by AIC), and stable mean estimates and CVs of MM_{3co} suggest an
549 adequately parametrized model. In addition, it is notable that including MM_{3co} is increasingly
550 beneficial for the narrow fit range as it leads to a significant reduction in the SD of the GABA+
551 estimates. This SD reduction is overserved for three models (Gauss_{fixed}, Gauss_{free}, MM09_{hard}) for
552 the wide fit range with 0.55 ppm baseline knot spacing and not overserved for the intermediate
553 fit range.

554

555 The different MM models in this study were based on certain assumptions, including the relative
556 contribution of MM_{3co} to the 3-ppm GABA peak to be around 50%^{1,6,8,19}. Levels of MM_{0,93} have
557 been found to be stable across the whole brain³⁶ and are thought to be stable across healthy sub-
558 jects. Under these assumptions, the MM09_{hard} model with a rigid amplitude coupling between
559 MM_{3co} and the non-overlapped MM_{0,93} peak is a suitable strategy, supported by favorable CVs
560 and Δ AIC. Further studies need to be performed to investigate the distribution and correlation
561 between MM_{0,93} and MM_{3co} in the brain. For the MM09_{soft} modeling strategy, we have found
562 the following MM_{3co}/MM_{0,93} ratios: 0.97 ± 0.29 (0.55 ppm baseline knot spacing), 0.88 ± 0.18
563 (0.4 ppm baseline knot spacing), and 0.95 ± 0.20 (0.25 ppm baseline knot spacing) compared to
564 0.66 for the composite MM09_{hard} model. This indicates higher ratios than expected in the initial

565 model parameters. However, true values can only be inferred from a large number of measured
566 macromolecular background spectra.

567

568 Compared to the Gauss_{fixed} model, the Gauss_{free} approach has one additional parameter to change
569 the FWHM of the MM_{3co} basis function. However, it can be assumed that difference in the
570 linewidth would mostly be accounted for by the Lorentzian linebroadening term. Therefore, only
571 minor differences in the fit results are expected, especially considering the high data quality in
572 this study. This was indeed the case in this study. As an example, for the wide fit range and
573 0.55 ppm baseline knot spacing, the FWHM of the MM_{3co} basis function was 14 Hz for the
574 Gauss_{fixed} model and 14.01 ± 0.10 Hz for the Gauss_{free} model.

575

576 Unedited MRSI data measured at 7T indicates significant differences between white and gray
577 matter for several macromolecules in the healthy brain³⁶. Changes in the MM concentrations dur-
578 ing disease may also affect the relative contribution to the 3-ppm peak, and therefore render
579 models with prior amplitude assumptions inaccurate. If there is reason to expect strong fluctua-
580 tions of MM_{3co}, a modeling strategy with fewer assumptions about amplitude ratios between the
581 metabolite of interest GABA or the MM_{0,93} signal and the MM_{3co} signal is preferable to the
582 MM09_{hard} strategy. Here, the Gauss_{free} and Gauss_{fixed} strategies could be used to account for
583 changes in the MM_{3co} contribution more freely, as their mean estimates of GABA and GABA+
584 were in good agreement with the more constrained approaches, although they led to increased
585 CVs and Δ AICs. In addition, the less-constrained models might be more appropriate for investi-
586 gating changes in MM_{3co} due to age³⁷ or disease, or for exploring frequency-drift-related effects
587 on the co-edited MM signal^{1,8,38}. Another potential way to model the co-edited MM signal is to
588 include lysine in the simulated basis set, as it has been identified as the potential source of the
589 signal⁶, although this approach would require appropriate broadening and incorporation of chem-
590 ical shift and coupling values from protein databases³⁹.

591

592 Overall, results did not differ drastically between modeling ranges, although it is noteworthy that
593 the effects of baseline flexibility were less pronounced for the narrow modeling range, likely be-
594 cause the complex interaction of the overlapping 2.25 ppm GABA and Glx signals with the un-
595 derlying baselines is omitted. Furthermore, there was no evidence that the intermediate modeling

596 range, which is proposed in the LCMModel manual¹⁸ to avoid frequently occurring co-edited lipid
597 signals, improved quantification substantially compared to both other modeling ranges, although
598 it should be mentioned that this particular dataset did not suffer from severe lipid contamination.
599 Taken together, the choice of modeling range does not impact quantitative results as substantially
600 as the inclusion of an MM model.

601
602 Baseline models are included in most LCM algorithms to account for signals not otherwise mod-
603 eled, e.g., residual water tails or unparametrized macromolecules and lipids. Compared to con-
604 ventional short-TE spectra, water and non-co-edited MMs are removed upon subtraction in the
605 GABA-edited spectrum, which is therefore frequently modeled with a stiffer baseline^{4,18}. Our
606 results show that sparser knot spacing (0.55 ppm) leads to lower CVs in metabolite estimates. A
607 more flexible baseline (0.25 ppm) improves local and global residuals, but not enough to justify
608 the additional model parameters (as per the AICs). More importantly, an overly flexible baseline
609 may absorb edited signal, although it appeared that it did not do so excessively even for the 0.25-
610 ppm strategies. The exception was the ‘none’ model, where the baseline was the only available
611 part of the model to take up signal, underlining the inadequacy of the default LCMModel approach.
612 Taken together, a relatively rigid baseline with a parametrized MM basis function is preferable
613 for LCM of GABA-edited spectra. A caveat to this recommendation is the observation of struc-
614 tural baseline fluctuations underneath the 2.25 ppm signals from GABA, Glx, GSH, NAA and
615 NAAG, particularly for the 0.25 ppm knot spacing and a relatively broad increase in the baseline
616 between 2.7 and 3.3 ppm. These were observed previously²⁷, and are likely signals from un-
617 parametrized MMs directly and indirectly affected by the editing pulse. Rigid baselines may
618 force a wrong metabolite model in that region and interfere with accurate estimation of GABA
619 and Glx. In fact, the structural Glx residual at 3.75 ppm suggests a systematic misestimation of
620 the Glx phase, likely driven by the 2.25 ppm signals. While beyond the scope of this investiga-
621 tion, it is conceivable that more informed parametrization (or, ideally, direct measurement) of
622 this unexplored MM background may benefit the modeling of the entire difference spectrum. Al-
623 ternatively, hitherto unexplored approaches with variable baseline knot spacing may be worth
624 investigating.

625

626 The HCar molecule has a GABA moiety with similar chemical shifts and is therefore co-edited.
627 Evidence regarding in-vivo HCar levels in the human brain is inconclusive – early work deter-
628 mined HCar levels to be 0.5 mM⁵ (compared to ~1 mM for GABA), while a recent hybrid up-
629 field/downfield inversion-recovery method determined the HCar/GABA ratio as 17%⁴⁰. There-
630 fore, we tested the impact of adding HCar to the basis set without additional constraints. Includ-
631 ing HCar systematically affected GABA and MM_{3co} estimates, in a way that strongly depended
632 on the choice of modeling range. HCar estimates themselves ranged from 2.2% to 19.1% of the
633 GABA+ signal, depending strongly on the degree of baseline flexibility. The results suggest that
634 the overlap between the three model terms (HCar, GABA, MM_{3co}) is too substantial for reliable
635 three-way separation, particularly in the presence of a highly flexible baseline. A minor increase
636 in “GABA+ plus HCar” estimates compared to GABA+ estimates was observed and the inclu-
637 sion of HCar did not substantially improve the CVs. Additionally, the disagreement between the
638 model and the data at 2.9 ppm indicates that a simple unconstrained addition of HCar to the
639 modeling is not justified.

640
641 Symmetric GABA-editing (edit-ON frequency at 1.9 ppm and edit-OFF frequency at 1.5 ppm) is
642 commonly used eliminate the MM_{3co} contamination of the 3-ppm GABA+ signal. In practice, B₀
643 instabilities lead to residual MM_{3co} components with variable polarity¹¹. The Gauss_{free} and
644 Gauss_{fixed} MM_{3co} models could potentially be used to account for those variable MM_{3co} contribu-
645 tions in those spectra. However, modeling of those spectra with the current strategies that do
646 have a non-negative model component as constraint would be challenging. Those modeling
647 strategies could potentially be adapted by using the B₀ history during the experiment³⁸ to predict
648 the polarity and relative amplitude of the MM_{3co} signal, and include those as a soft constraint rel-
649 ative to the MM₀₉ signal (MM_{09_{hard}} or MM_{09_{soft}}) or the GABA signal (GABA_{hard} or GABA_{soft}).

650 Limitations

651 A limitation of this study is the high spectral quality (SNR, linewidth, no apparent subtraction
652 artefacts, or lipid contaminations) of the dataset analyzed. We did not investigate model
653 parametrizations of movement or drift, which may introduce systematic changes to the co-edited
654 MM signal. While our results suggest that using the wide modeling range with a rigid baseline is
655 beneficial, strong co-edited lipid signals are likely to not be modeled appropriately, and the in-

656 intermediate modeling range may be more suitable. Further studies of the possible impact of
657 changes in spectral quality need to be performed to validate the modeling strategies under subop-
658 timal conditions.

659

660 Another limitation is that there is no ‘gold standard’ of metabolite level estimation in GABA-
661 edited MRS to validate the results against. The performance of different algorithms or in this
662 study modeling strategy is often judged by the level of variance²⁶. A lower variance does, of
663 course, not necessarily reflect greater modeling accuracy, but under the assumption that the ho-
664 mogeneous study population and data acquisition contribute comparably little biological and in-
665 strumental variance, CVs will predominantly reflect variance introduced by the modeling ap-
666 proach. Recently, the field is witnessing increasing efforts to generate simulated spectra with
667 known ground truth as a gold standard, although these approaches can only be successful to the
668 extent that those spectra are truly representative of in-vivo data^{41–43}. Further, such gold standard
669 studies with a known ground truth could be used to validate whether a correct separation of
670 GABA and MM_{3co} is achievable by advanced LCM. This study indicates a low-to-moderate cor-
671 relation between the GABA and MM_{3co} estimates, suggesting that the two components are not
672 reliably separated. However, some of the modeling strategies appeared to have a lower associa-
673 tion between both estimates and could possibly be validated further on a synthetic dataset with
674 known GABA and MM_{3co} concentrations.

675

676 AIC as a measure of the goodness of fit can be used for linear and non-linear approaches if the
677 log-likelihood is obtained similarly. However, there are two potential limitations for the applica-
678 tion of AIC in this study. First, for linear-combination modeling of MRS data, as implemented in
679 Osprey, a non-linear optimization is followed by a linear optimization during each iteration. Pa-
680 rameters are treated equally in the calculation of the AIC regardless of whether they are non-
681 linear (e.g., a phase parameter) or linear (an amplitude parameter). Second, the AIC penalizes
682 complex models, but does not measure effects of soft constraints and is likely to prefer models
683 without a soft constraint as those should have a reduced likelihood⁴⁴. Here, we introduced a ra-
684 ther arbitrary correction term of 0.5 per soft constraint for those models to reduce this effect.
685 Therefore, the resulting Δ AIC values in this study should be interpreted with care and considered
686 as only one among several metrics to evaluate model performance.

687 **Conclusion**

688 This study proposed and compared different modeling strategies for LCM of GABA+-edited dif-
689 ference spectra from a multi-site MEGA-PRESS dataset. Introducing a parametrized model for
690 co-edited macromolecules reduces fit residuals, while maintaining low coefficients of variation
691 of GABA+ estimates. A rigid baseline was found to be beneficial, while using a narrower model-
692 ing range did not significantly improve the modeling. The overall modeling results suggest that
693 GABA-edited data are reliably modeled with an adequately parametrized MM_{3co} model, con-
694 strained by the non-overlapped 0.93-ppm MM resonance, in combination with a full modeling
695 range (between 0.5 and 4 ppm) and sparse knot spacing (0.55 ppm). Incorporating
696 homocarnosine into the modeling did not significantly improve the GABA+ estimates and did
697 not allow for a stable separation of GABA and HCar.

698 **References**

- 699 1. Choi I-Y, Andronesi OC, Barker P, et al. Spectral editing in ¹H magnetic resonance spec-
700 troscopy: Experts' consensus recommendations. *NMR Biomed.* 2021;n/a(n/a):e4411.
701 doi:<https://doi.org/10.1002/nbm.4411>
- 702 2. Edden RAE, Puts NAJ, Harris AD, Barker PB, Evans CJ. Gannet: A batch-processing tool
703 for the quantitative analysis of gamma-aminobutyric acid-edited MR spectroscopy spectra.
704 *J Magn Reson Imaging.* 2014;40(6):1445-1452. doi:10.1002/jmri.24478
- 705 3. Wilson M, Reynolds G, Kauppinen RA, Arvanitis TN, Peet AC. A constrained least-
706 squares approach to the automated quantitation of in vivo ¹H magnetic resonance spectros-
707 copy data. *Magn Reson Med.* 2011;65(1):1-12.
- 708 4. Provencher SW. Automatic quantitation of localized in vivo ¹H spectra with LCModel.
709 *NMR Biomed.* 2001;14(4):260-264. doi:10.1002/nbm.698
- 710 5. Petroff OAC, Hyder F, Rothman DL, Mattson RH. Topiramate Rapidly Raises Brain
711 GABA in Epilepsy Patients. *Epilepsia.* 2001;42(4):543-548.
712 doi:<https://doi.org/10.1046/j.1528-1157.2001.18800.x>
- 713 6. Deelchand DK, Marjańska M, Henry P-G, Terpstra M. MEGA-PRESS of GABA+: Influ-
714 ences of acquisition parameters. *NMR Biomed.* 2019;n/a(n/a):e4199.
715 doi:<https://doi.org/10.1002/nbm.4199>
- 716 7. Marjańska M, Terpstra M. Influence of fitting approaches in LCModel on MRS quantifica-
717 tion focusing on age-specific macromolecules and the spline baseline. *NMR Biomed.* No-
718 vember 2019. doi:10.1002/nbm.4197
- 719 8. Shungu DC, Mao X, Gonzales R, et al. Brain γ -aminobutyric acid (GABA) detection in vi-
720 vo with the J-editing (¹H) MRS technique: a comprehensive methodological evaluation of
721 sensitivity enhancement, macromolecule contamination and test-retest reliability. *NMR Bi-*
722 *omed.* 2016;29(7):932-942. doi:10.1002/nbm.3539
- 723 9. Bhagwagar Z, Wylezinska M, Jezzard P, et al. Reduction in Occipital Cortex γ -
724 Aminobutyric Acid Concentrations in Medication-Free Recovered Unipolar Depressed and
725 Bipolar Subjects. *Biol Psychiatry.* 2007;61(6):806-812. doi:10.1016/j.biopsych.2006.08.048
- 726 10. Mikkelsen M, Barker PB, Bhattacharyya PK, et al. Big GABA: Edited MR spectroscopy at
727 24 research sites. *NeuroImage.* 2017;159:32-45. doi:10.1016/j.neuroimage.2017.07.021
- 728 11. Edden RAE, Oeltzschner G, Harris AD, et al. Prospective frequency correction for macro-
729 molecule-suppressed GABA editing at 3T. *J Magn Reson Imaging JMRI.* 2016;44(6):1474-
730 1482. doi:10.1002/jmri.25304
- 731 12. Oeltzschner G, Zöllner HJ, Hui SCN, et al. Osprey: Open-source processing, reconstruction
732 & estimation of magnetic resonance spectroscopy data. *J Neurosci Methods.*
733 2020;343:108827. doi:10.1016/j.jneumeth.2020.108827

- 734 13. Osprey GitHub repository. Osprey GitHub repository.
735 <https://github.com/schorschinho/osprey>. Published 2020. Accessed May 27, 2020.
- 736 14. Klose U. In vivo proton spectroscopy in presence of eddy currents. *Magn Reson Med*.
737 1990;14(1):26-30. doi:10.1002/mrm.1910140104
- 738 15. Mikkelsen M, Tapper S, Near J, Mostofsky SH, Puts NAJ, Edden RAE. Correcting fre-
739 quency and phase offsets in MRS data using robust spectral registration. *NMR Biomed*. July
740 2020:e4368. doi:10.1002/nbm.4368
- 741 16. Barkhuijsen H, de Beer R, van Ormondt D. Improved algorithm for noniterative time-
742 domain model fitting to exponentially damped magnetic resonance signals. *J Magn Reson*
743 1969. 1987;73(3):553-557. doi:10.1016/0022-2364(87)90023-0
- 744 17. Simpson R, Devenyi GA, Jezzard P, Hennessy TJ, Near J. Advanced processing and simu-
745 lation of MRS data using the FID appliance (FID-A)—An open source, MATLAB-based
746 toolkit. *Magn Reson Med*. 2017;77(1):23-33. doi:10.1002/mrm.26091
- 747 18. Provencher S. LCMModel & LCMgui User's Manual. LCMModel & LCMgui User's Manual.
748 <http://s-provencher.com/pub/LCMModel/manual/manual.pdf>. Published 2020. Accessed April
749 28, 2020.
- 750 19. Henry PG, Dautry C, Hantraye P, Bloch G. Brain gaba editing without macromolecule con-
751 tamination. *Magn Reson Med*. 2001;45(3):517-520. doi:10.1002/1522-
752 2594(200103)45:3<517::AID-MRM1068>3.0.CO;2-6
- 753 20. Levenberg K. A method for the solution of certain non-linear problems in least squares. *Q*
754 *Appl Math*. 1944;2(2):164-168. doi:10.1090/qam/10666
- 755 21. Marquardt DW. An Algorithm for Least-Squares Estimation of Nonlinear Parameters. *J Soc*
756 *Ind Appl Math*. 1963;11(2):431-441. doi:10.1137/0111030
- 757 22. Becker S. LBFGSB (L-BFGS-B) mex wrapper - File Exchange - MATLAB Central.
758 LBFGSB (L-BFGS-B) mex wrapper - File Exchange - MATLAB Central.
759 [https://www.mathworks.com/matlabcentral/fileexchange/35104-lbfgsb-l-bfgs-b-mex-](https://www.mathworks.com/matlabcentral/fileexchange/35104-lbfgsb-l-bfgs-b-mex-wrapper)
760 [wrapper](https://www.mathworks.com/matlabcentral/fileexchange/35104-lbfgsb-l-bfgs-b-mex-wrapper). Published February 23, 2015. Accessed March 3, 2021.
- 761 23. Byrd RH, Lu P, Nocedal J, Zhu C. A Limited Memory Algorithm for Bound Constrained
762 Optimization. *SIAM J Sci Comput*. 1995;16(5):1190-1208. doi:10.1137/0916069
- 763 24. Zhu C, Byrd RH, Lu P, Nocedal J. Algorithm 778: L-BFGS-B: Fortran subroutines for
764 large-scale bound-constrained optimization. *ACM Trans Math Softw*. 1997;23(4):550-560.
765 doi:10.1145/279232.279236
- 766 25. Wilson M, Andronesi O, Barker PB, et al. *Methodological Consensus on Clinical Proton*
767 *MRS of the Brain: Review and Recommendations*. Vol 82. John Wiley and Sons Inc.; 2019.
768 doi:10.1002/mrm.27742

- 769 26. Zöllner HJ, Považan M, Hui SCN, Tapper S, Edden RAE, Oeltzschner G. Comparison of
770 different linear-combination modeling algorithms for short-TE proton spectra. *NMR Bio-*
771 *med.* 2021;n/a(n/a):e4482. doi:<https://doi.org/10.1002/nbm.4482>
- 772 27. Murdoch JB, Dydak U. Modeling MEGA-PRESS macromolecules for a better grasp of
773 GABA. In: *19th Annual Meeting of the International Society for Magnetic Resonance in*
774 *Medicine (ISMRM)*. ; 2011.
775 [https://scholar.google.com/scholar_lookup?title=Modeling%20MEGA-](https://scholar.google.com/scholar_lookup?title=Modeling%20MEGA-PRESS%20macromolecules%20for%20a%20better%20grasp%20of%20GABA&publication_year=2011&author=J.B.%20Murdoch&author=U.%20Dydak)
776 [PRESS%20macromolecules%20for%20a%20better%20grasp%20of%20GABA&publicatio](https://scholar.google.com/scholar_lookup?title=Modeling%20MEGA-PRESS%20macromolecules%20for%20a%20better%20grasp%20of%20GABA&publication_year=2011&author=J.B.%20Murdoch&author=U.%20Dydak)
777 [n_year=2011&author=J.B.%20Murdoch&author=U.%20Dydak](https://scholar.google.com/scholar_lookup?title=Modeling%20MEGA-PRESS%20macromolecules%20for%20a%20better%20grasp%20of%20GABA&publication_year=2011&author=J.B.%20Murdoch&author=U.%20Dydak). Accessed July 1, 2020.
- 778 28. Dydak U, Jiang YM, Long LL, et al. In vivo measurement of brain GABA concentrations
779 by magnetic resonance spectroscopy in smelters occupationally exposed to manganese. *En-*
780 *viron Health Perspect.* 2011;119(2):219-224. doi:10.1289/ehp.1002192
- 781 29. R Core Team. *R: A Language and Environment for Statistical Computing*. Vienna, Austria:
782 R Foundation for Statistical Computing; 2017. <https://www.R-project.org/>.
- 783 30. SpecVis GitHub repository. SpecVis GitHub repository.
784 <https://github.com/hezoe100/SpecVis>. Published 2020. Accessed May 27, 2020.
- 785 31. Wickham H. *Ggplot2: Elegant Graphics for Data Analysis*. Springer-Verlag New York;
786 2009. <http://ggplot2.org>.
- 787 32. Zöllner HJ. Comparison of linear-combination modeling strategies for GABA-edited MRS
788 at 3T. <https://osf.io/aqm8f/>. Published April 30, 2021. Accessed April 30, 2021.
- 789 33. Akaike H. A new look at the statistical model identification. *IEEE Trans Autom Control.*
790 1974;19(6):716-723. doi:10.1109/TAC.1974.1100705
- 791 34. Mikkelsen M, Rimbault DL, Barker PB, et al. Big GABA II: Water-referenced edited MR
792 spectroscopy at 25 research sites. *NeuroImage.* 2019;191:537-548.
793 doi:10.1016/J.NEUROIMAGE.2019.02.059
- 794 35. Cudalbu C, Behar KL, Bhattacharyya PK, et al. Contribution of macromolecules to brain
795 ¹H MR spectra: Experts' consensus recommendations. *NMR Biomed Revis.* 2020.
- 796 36. Považan M, Strasser B, Hangel G, et al. Simultaneous mapping of metabolites and individ-
797 ual macromolecular components via ultra-short acquisition delay ¹H MRSI in the brain at
798 7T. *Magn Reson Med.* 2018;79(3):1231-1240. doi:10.1002/mrm.26778
- 799 37. Marjańska M, Deelchand DK, Hodges JS, et al. Altered macromolecular pattern and con-
800 tent in the aging human brain. *NMR Biomed.* 2018;31(2):e3865. doi:10.1002/nbm.3865
- 801 38. Veen JW van der, Marengo S, Berman KF, Shen J. Retrospective correction of frequency
802 drift in spectral editing: The GABA editing example. *NMR Biomed.* 2017;30(8):e3725.
803 doi:<https://doi.org/10.1002/nbm.3725>

- 804 39. Borbath T, Manohar SM, Henning A. Towards a Fitting Model of Macromolecular Spectra:
805 Amino Acids. In: *27th Annual Meeting of the International Society for Magnetic Resonance*
806 *in Medicine (ISMRM)*. Montreal, Canada; 2019.
- 807 40. Landheer K, Prinsen H, Petroff OA, Rothman DL, Juchem C. Elevated homocarnosine and
808 GABA in subject on isoniazid as assessed through ¹H MRS at 7T. *Anal Biochem*.
809 2020;599:113738. doi:10.1016/j.ab.2020.113738
- 810 41. Bolliger CS, Boesch C, Kreis R. On the use of Cramér–Rao minimum variance bounds for
811 the design of magnetic resonance spectroscopy experiments. *NeuroImage*. 2013;83:1031-
812 1040. doi:10.1016/j.neuroimage.2013.07.062
- 813 42. Landheer K, Gajdošík M, Juchem C. A semi-LASER, single-voxel spectroscopic sequence
814 with a minimal echo time of 20.1 ms in the human brain at 3 T. *NMR Biomed*.
815 2020;33(9):e4324. doi:10.1002/nbm.4324
- 816 43. Hui SCN, Mikkelsen M, Zöllner HJ, et al. Frequency drift in MR spectroscopy at 3T.
817 *NeuroImage*. 2021;241:118430. doi:10.1016/j.neuroimage.2021.118430
- 818 44. Endres DM, Chiovetto E, Giese M. Model selection for the extraction of movement primi-
819 tives. *Front Comput Neurosci*. 2013;7. doi:10.3389/fncom.2013.00185
- 820

Supplementary Material

Table of Contents

1. List of included subjects
2. Macro-molecule function definitions
3. Mean and SD spectra as well as individual spectra
4. Statistics - GABA estimates
5. Statistics - MM_{3co} estimates
6. Model overview basis set with homocarnosine
7. Distribution of GABA+ and homocarnosine

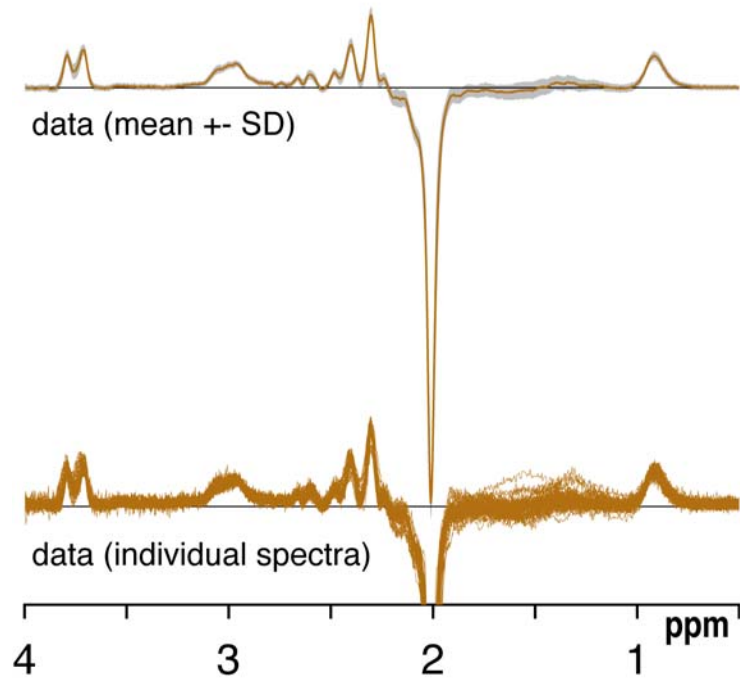
Supplementary Material 1 – List of included subjects. All datasets are available at <https://www.nitrc.org/projects/biggabe/>

site	subjects	Σ
P01	S01,S03,S04,S05,S08	5
P03	S02,S03,S04,S07,S08,S09,S10,S11,S12	9
P05	S01,S02,S03,S05,S06,S07,S08	7
P06	S01,S02,S03,S04,S05,S06,S07,S08,S09	9
P07	S02,S03,S04,S09,S10,S11,S12	7
P08	S01,S02,S03,S04,S05,S06,S07,S08,S09,S10,S11,S12	12
P09	S01,S02,S03,S04,S05,S06,S07,S08,S09,S10,S11,S12	12
Σ = 7		Σ = 61

Supplementary Material 2. *Properties of the Gaussian functions of the broad macromolecule and lipid resonances included in the basis sets, taken from section 11.7 of the LCMoDel manual. The amplitude values are scaled relative to the CH₃ singlet of creatine with amplitude 3.*

<i>Name</i>	<i>Frequencies [ppm]</i>	<i>FWHM [ppm]</i>	<i>Amplitude</i>
<i>edit-OFF spectrum basis set</i>			
MM _{0.94}	0.915	0.14	3.00
MM _{1.22}	1.22	0.15	2.00
MM _{1.43}	1.43	0.17	2.00
MM _{1.70}	1.67	0.15	0.20
MM _{2.05}	2.08	0.15	1.33
	2.25	0.20	0.33
	1.95	0.15	0.33
	3.00	0.20	0.40
Lip09	0.89	0.14	3.00
Lip13	1.28	0.15	2.00
	1.28	0.089	2.00
Lip20	2.04	0.15	1.33
	2.25	0.15	0.67
	2.80	0.20	0.87
<i>Difference spectrum basis set</i>			
MM _{0.94}	0.915	0.14	3
MM _{3co}	3	14 Hz	2

Data overview



Supplementary Material 3 – Overview of the processed data including the mean \pm SD and individual data.

Supplementary Material 4 – GABA mean and SDs for all modeling strategies (ratios to tCr). Significant differences ($p < .05$) between the corresponding model and the ‘none’ model (gray shade) are indicated in bold.

modeling range		narrow			intermediate			wide		
knot spacing (ppm)		0.55	0.4	0.25	0.55	0.4	0.25	0.55	0.4	0.25
none	[GABA]	0.220	0.213	0.193	0.297	0.186	0.204	0.284	0.288	0.158
		<i>.062</i>	<i>.071</i>	<i>.057</i>	<i>.048</i>	<i>.061</i>	<i>.044</i>	<i>.029</i>	<i>.034</i>	<i>.066</i>
GABA _{hard}	[GABA]	0.164	0.146	0.156	0.207	0.148	0.165	0.194	0.207	0.150
		<i>.021</i>	<i>.02</i>	<i>.023</i>	<i>.024</i>	<i>.031</i>	<i>.021</i>	<i>.021</i>	<i>.023</i>	<i>.034</i>
GABA _{soft}	[GABA]	0.108	0.102	0.108	0.207	0.130	0.148	0.203	0.204	0.115
		<i>.024</i>	<i>.027</i>	<i>.025</i>	<i>.048</i>	<i>.039</i>	<i>.03</i>	<i>.026</i>	<i>.027</i>	<i>.049</i>
Gauss _{fixed}	[GABA]	0.074	0.080	0.081	0.174	0.106	0.118	0.136	0.145	0.108
		<i>.031</i>	<i>.031</i>	<i>.035</i>	<i>.055</i>	<i>.045</i>	<i>.045</i>	<i>.031</i>	<i>.032</i>	<i>.068</i>
Gauss _{free}	[GABA]	0.079	0.078	0.081	0.180	0.107	0.119	0.137	0.145	0.107
		<i>.034</i>	<i>.032</i>	<i>.033</i>	<i>.054</i>	<i>.050</i>	<i>.045</i>	<i>.033</i>	<i>.031</i>	<i>.069</i>
MM09 _{hard}	[GABA]	-	-	-	-	-	-	0.195	0.189	0.106
								<i>.034</i>	<i>.032</i>	<i>.060</i>
MM09 _{soft}	[GABA]	-	-	-	-	-	-	0.152	0.154	0.098
								<i>.03</i>	<i>.031</i>	<i>.072</i>

Supplementary Material 5 – MM_{3co} mean and SDs for all modeling strategies (ratios to tCr). Significant differences ($p < .05$) between the corresponding model and GABA_{soft} model (gray shade) are indicated in bold.

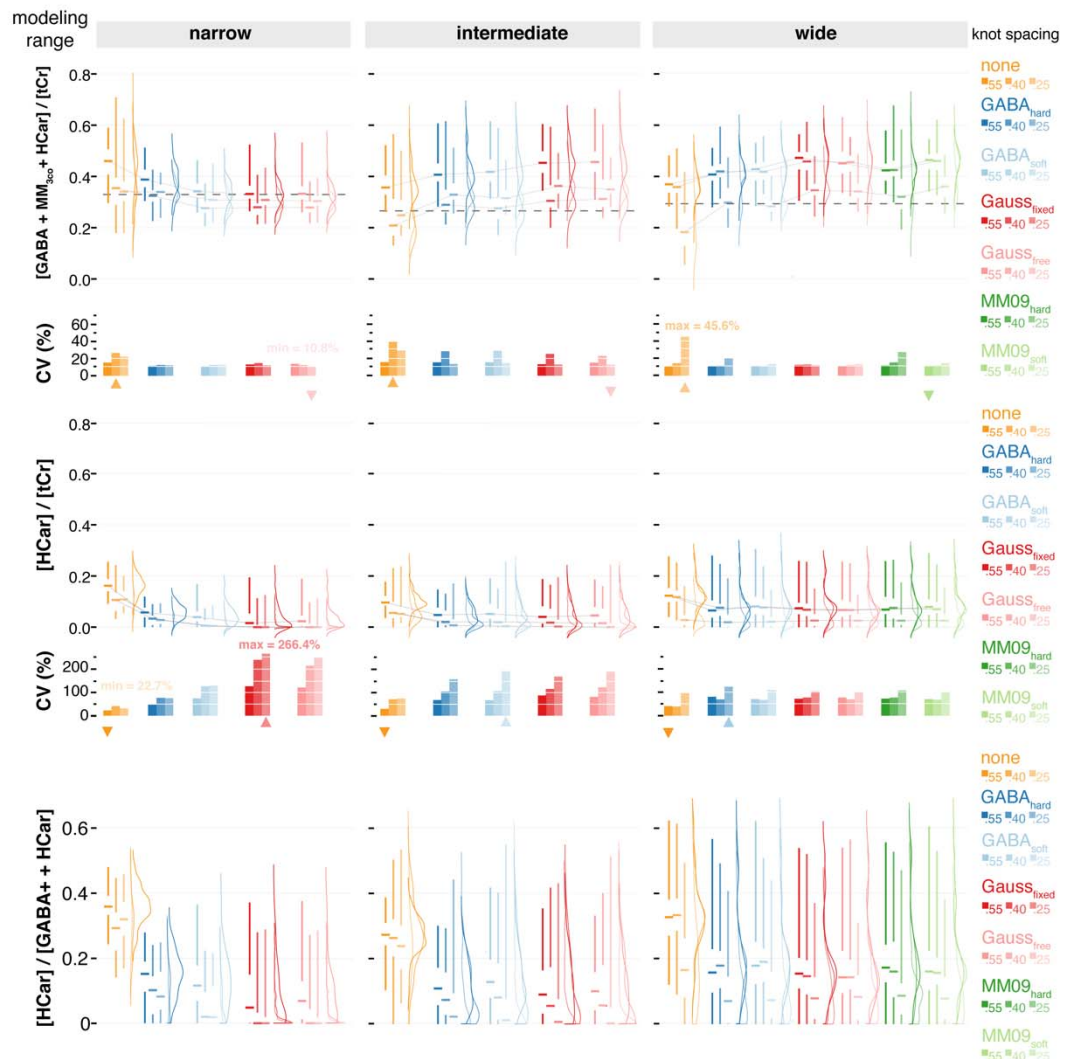
modeling range	narrow	intermediate	wide
----------------	--------	--------------	------

knot spacing (ppm)		0.55	0.4	0.25	0.55	0.4	0.25	0.55	0.4	0.25
none	[MM _{3co}]	-	-	-	-	-	-	-	-	-
GABA_{hard}	[MM _{3co}]	-	-	-	-	-	-	-	-	-
GABA_{soft}	[MM _{3co}]	0.19 .026	0.165 .025	0.186 .027	0.210 .038	0.148 .033	0.175 .024	0.172 .039	0.194 .032	0.156 .032
Gauss_{fixed}	[MM _{3co}]	0.233 .039	0.192 .038	0.223 .041	0.237 .048	0.192 .03	0.215 .035	0.233 .054	0.237 .045	0.235 .053
Gauss_{free}	[MM _{3co}]	0.226 .038	0.198 .036	0.22 .045	0.229 .044	0.193 .031	0.213 .035	0.227 .057	0.237 .042	0.234 .053
MM09_{hard}	[MM _{3co}]	-	-	-	-	-	-	0.201 .032	0.232 .043	0.240 .040
MM09_{soft}	[MM _{3co}]	-	-	-	-	-	-	0.216 .051	0.232 .037	0.240 .045



Supplementary Material 6 – Mean modeling results and homocarnosine estimates for all modeling strategies with homocarnosine. A substantial structured residual is visible at 3 ppm if for all modeling strategies and for the narrow and intermediate modeling range the homocarnosine concentrations are significantly lower compared to omitting the co-edited MM, especially for knot spacings ≤ 0.4 ppm. All

three modeling ranges (columns), three spline knot spacings (rows), and MM_{3co} model (color-coded) are presented with mean residuals and fits, as well as the GABA, MM_{3co} , homocarnosine (HCar) and spline baseline models. The mean data is included in black. The arrows indicate the range of values for a specific modeling range and spline knot spacing with the color corresponding to the MM_{3co} model with minimum/maximum value.



Supplementary Material 7 - Distribution of GABA+ plus HCar and HCar estimates and the relative contribution of HCar to GABA+ plus HCar for all modeling strategies. The mean estimates of GABA+ plus HCar across the three spline knot spacings of the 'none' approach are indicated as a dashed line for each modeling range. All three modeling ranges (column) and three spline knot spacings (within each column), and MM_{3co} models (color-coded) are presented. Distributions are shown as half-violins

(smoothed distribution), box plots with median, interquartile range, and 25th/75th quartile. The median lines of the box plots are connected to visualize trends within a specific baseline knot spacing. CVs are summarized as bar plots. Minimum/maximum CVs for each spline knot spacing are indicated as downwards/upwards triangles in the color corresponding to the MM_{3co} model. Global minimum and maximum CVs across all models are added as text.

Declaration of competing interests

The authors have nothing to declare.

Acknowledgement

This work is supported by NIH grants P41 EB031771, R01 EB016089, R01 EB023963, R01 EB028259, R21 AG060245, and K99/R00 AG062230.

CRediT authorship contribution statement

Helge J. Zöllner: Software, Formal Analysis, Investigation, Writing – Original Draft, Writing – Review & Editing, Visualization. **Sofie Tapper:** Investigation, Writing – Review & Editing. **Steve C. N. Hui:** Investigation, Writing – Review & Editing. **Richard A. E. Edden:** Conceptualization, Formal Analysis, Writing – Review & Editing, Supervision, Project administration, Funding acquisition. **Peter B. Barker:** Writing – Review & Editing, Supervision, Funding acquisition. **Georg Oeltzschner:** Conceptualization, Methodology, Software, Investigation, Formal Analysis, Writing – Review & Editing, Supervision, Funding acquisition.